Polar Geosci., **14**, 1–24, 2001

Ultrahigh temperature sapphirine-osumilite and sapphirine-quartz granulites from Bunt Island in the Napier Complex, East Antarctica —Reconnaissance estimation of *P-T* evolution—

Yasuhito Osanai[1], Tsuyoshi Toyoshima[2], Masaaki Owada[3], Toshiaki Tsunogae[4], Tomokazu Hokada[5,*], Warwick A. Crowe[6] and Isao Kusachi[1]

[1]*Department of Earth Sciences, Okayama University, Tsushima-naka 3-1-1, Okayama 700-8530 (osanai@cc.okayama-u.ac.jp)*
[2]*Department of Geology, Niigata University, Ikarashi 2-chome, Niigata 950-2181*
[3]*Department of Earth Sciences, Yamaguchi University, Yoshida 1677-1, Yamaguchi 753-8512*
[4]*Institute of Geoscience, University of Tsukuba, Tennoudai 1-1-1, Tsukuba 305-8571*
[5]*National Institute of Polar Research, Kaga 1-chome, Itabashi-ku, Tokyo 173-8515*
[6]*Department of Geology and Geophysics, University of Western Australia, Nedlands, Perth 6907, Australia*

Abstract: The summer party of the 39th Japanese Antarctic Research Expedition (1997–1998) carried out geological field work on Bunt Island at the southeastern end of Amundsen Bay, Enderby Land, which is in the highest-grade metamorphic region in the Napier Complex. The island is underlain by various kinds of ultrahigh-temperature (UHT) metamorphic rocks including osumilite-bearing aluminous sapphirine-garnet-orthopyroxene granulite and quartz-predominant sapphirine-garnet-sillimanite gneiss containing the assemblage sapphirine-quartz.

Osumilite-bearing aluminous granulite is silica-undersaturated, aluminous and magnesian chromium-rich chemical affinity. Osumilite-bearing granulite from Bunt Island could be formed through the mixing of clayey materials or other felsic components derived from felsic igneous rocks with a relatively high proportion of mafic to ultramafic detritus in the sedimentary precursor. The chemical mixing could have taken place during *c.* 3.2 and *c.* 2.5 Ga. *P-T* estimation for osumilite-bearing granulite and related sapphirine-quartz gneiss indicates ultrahigh-temperature condition (~1100°C, ~1100 MPa) as well as other high-grade rocks from the Napier Complex, but the rocks from Bunt Island clearly show isothermal decompression in part of the clockwise *P-T* evolutional process.

key words: sapphirine, osumilite, *P-T* path, Bunt Island, Napier Complex

1. Introduction

The Napier Complex in northern Enderby Land, East Antarctica is one of the most famous regional ultrahigh-temperature (UHT) metamorphic terranes in the world.

* Present address: Department of Geology, National Science Museum, 3-23-1 Hyakunin-cho, Shinjuku-ku, Tokyo 169-0073.

Especially in the last two decades, geological investigations, including petrology and geochronology, have been carried out over an extended area of the Napier Complex (*e.g.* Sheraton *et al.*, 1987). The dominant rock types of the Napier Complex are orthopyroxene- and garnet-bearing quartzofeldspathic gneisses of igneous origin (Archaean TTG-type tonalitic orthogneiss) with subordinate constituents of ultramafic, mafic, pelitic, calcareous, siliceous and aluminous granulites. Some of these gneisses and granulites are characterized by UHT-type mineral assemblages of spinel+quartz and garnet+sapphirine+quartz, with or without orthopyroxene and osumilite, and orthopyroxene+sillimanite+quartz (*e.g.* Dallwitz, 1968; Sheraton, 1980; Sheraton *et al.*, 1987; Ellis, 1980; Ellis *et al.*, 1980; Grew, 1980, 1982; Harley, 1985, 1987, 1998; Sandiford, 1985; Motoyoshi and Matsueda, 1984; Motoyoshi and Hensen, 1989; Motoyoshi *et al.*, 1990, 1994, 1995; Ishizuka *et al.*, 1998; Osanai *et al.*, 1999; Hokada *et al.*, 1999; Yoshimura *et al.*, 2000). The metamorphic evolution of the highest-grade metamorphic rocks in the Napier Complex has been considered to have peaked at *c.* 1000 MPa and *c.* 1100°C or higher followed by near-isobaric cooling (IBC) (*e.g.* Harley and Motoyoshi, 2000). But unfortunately the prograde metamorphic evidence is rarely preserved and remains poorly understood.

During the 1997–1998 austral summer season, a geological team belonging to the 39th Japanese Antarctic Research Expedition (JARE-39) carried out a geological survey on Bunt Island and Tonagh Island (*e.g.* Osanai *et al.*, 1999) as part of the Japanese earth science project "SEAL" (Structure and Evolution of east Antarctic Lithosphere). Bunt

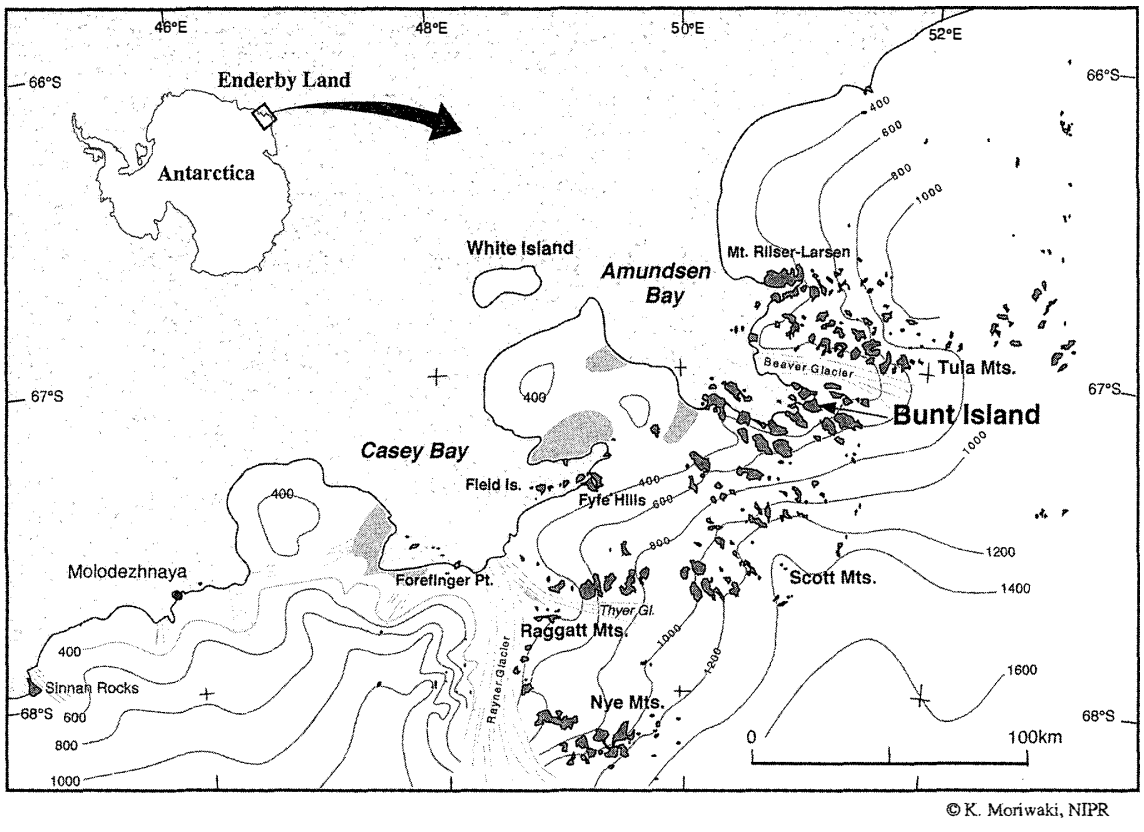

Fig. 1. Location of Bunt Island in Enderby Land, East Antarctica.

Island is located in Amundsen Bay (Fig. 1), where characteristic UHT-metamorphic rocks such as osumilite-bearing aluminous sapphirine granulite and quartzofeldspathic gneiss containing sapphirine-quartz direct association are widely exposed. In this paper we describe new petrographical and mineralogical data of UHT-metamorphic rocks from Bunt Island in the Napier Complex and interpret their implications for metamorphic evolution.

2. Geological setting

Bunt Island is located at the southeastern end of Amundsen Bay in Enderby Land, which belongs to the central Napier Complex, and is *c.* 30 km east from Tonagh Island

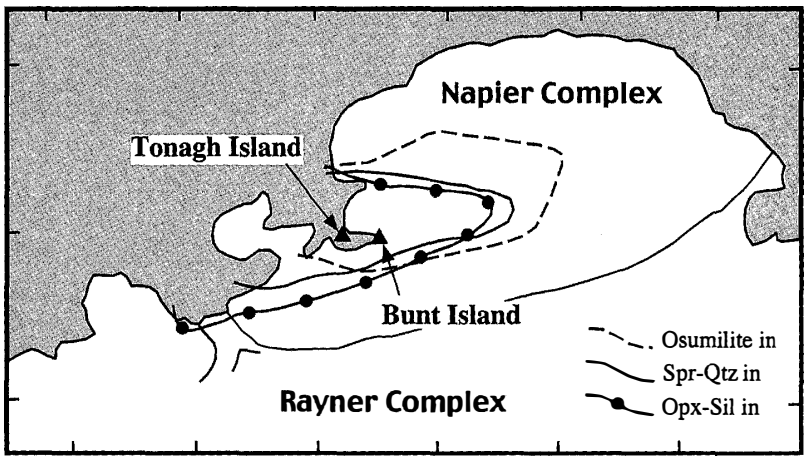

Fig. 2. Highest-grade region of the Napier Complex. Bunt and Tonagh Islands are situated within the region surrounded by the isograds "osumilite in", "sapphirine-quartz in" and "orthopyroxene-sillimanite in", after Harley and Hensen (1990).

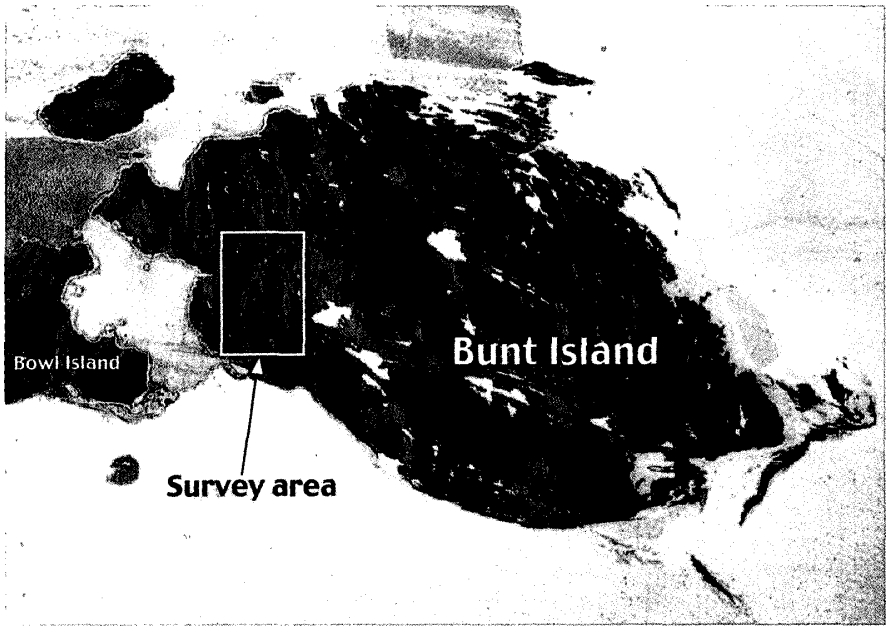

Fig. 3. Survey area in Bunt Island, where well layered structure is clearly observed.

(Fig. 1). The island is situated in the highest-grade metamorphic region of the Napier Complex, above the osumilite-in, sapphirine+quartz-in and orthopyroxene+sillimanite-in isograds (Grew, 1982; Sheraton *et al.*, 1987; Harley and Hensen, 1990) (Fig. 2). There

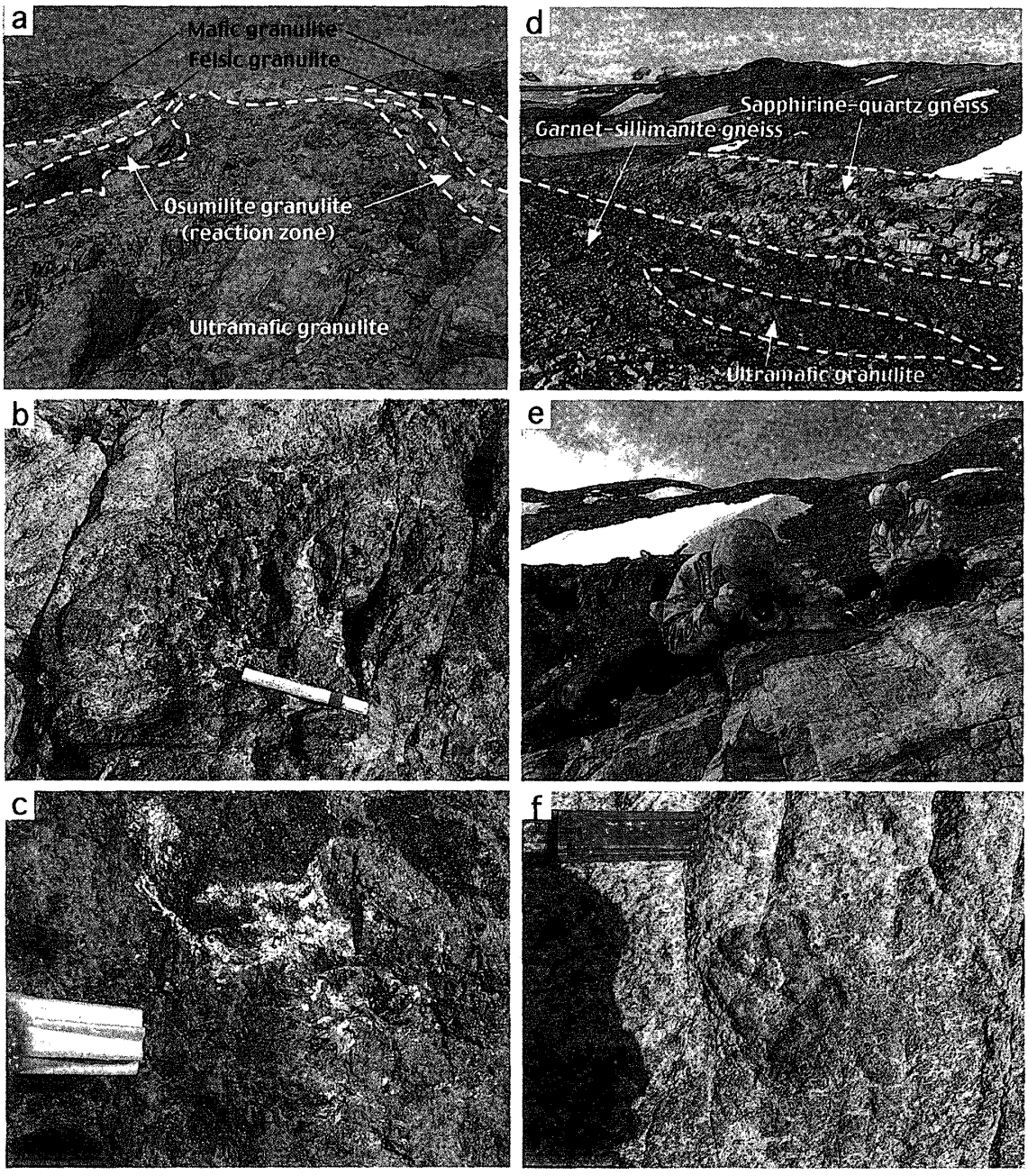

Fig. 4. Modes of occurrence of osumilite-bearing aluminous granulite and sapphirine-quartz gneiss. a: Osumilite granulite occurs between ultramafic granulite (garnet-bearing orthopyroxenite) and surrounding garnet-bearing felsic granulite. b: Boundary between osumilite-orthopyroxene-garnet-sapphirine granulite (central portion) and garnet-bearing felsic granulite (upper portion). c: Closeup view of osumilite (brilliant white) and garnet association. d: Layered sapphirine-quartz gneiss, e: Thin alternation of garnet-rich and garnet-poor parts in sapphirine-quartz gneiss, f: Closeup view of porphyroblastic garnet-bearing sapphirine-quartz gneiss.

have not been any previous detailed geological investigations, even by Australian expeditions (*e.g.* Sheraton *et al.*, 1987). We focused the geological survey in the western part of Bunt Island (Fig. 3). The studied rocks in Bunt Island are clearly different from the metamorphic suite on Tonagh Island, where detailed geological investigations have been carried out by JARE parties. According to Sheraton *et al.* (1987), Bunt and Tonagh Islands are underlain by layered garnet-quartz-feldspar gneiss with subordinate pelitic, psammitic and ferruginous metasediments (the Tula Series of Kamenev, 1975). However, Bunt Island differs from Tonagh Island, because there is no evidence for a Proterozoic metamorphic event (Rayner metamorphism) on Bunt Island (Sheraton *et al.*, 1987), but not only Archaean Napier metamorphism; but the effect of Rayner metamorphism can also be identified at Tonagh Island (Owada *et al.*, 2001; Osanai *et al.*, 2001). Therefore Bunt Island is more suitable for studying ultrahigh-temperature metamorphism.

The investigated area in Bunt Island (Fig. 3) is underlain by layered gneiss containing garnet-bearing and orthopyroxene-bearing quartzofeldspathic gneisses as abundant lithofacies with subordinate intercalations of two pyroxene-bearing mafic granulite, metamorphosed ultramafic rocks (ultramafic granulite), garnet-sillimanite gneiss and aluminous granulites (Fig. 4). Ultramafic granulite characteristically forms elongated lenses or blocks, which could be derived by boudinage of an ultramafic intrusion or dike with komatiitic composition (Owada *et al.*, 1999; Osanai *et al.*, 2001). The layered units form a homocline striking from NNW-SSE to NW-SE and gently dipping E (30°– 40°E). Preferred orientation of metamorphic minerals (foliation, lineation) is generally quite weak or altogether absent.

Rocks containing diagnostic UHT-mineral assemblages at Bunt Island have the following two modes of occurrence:

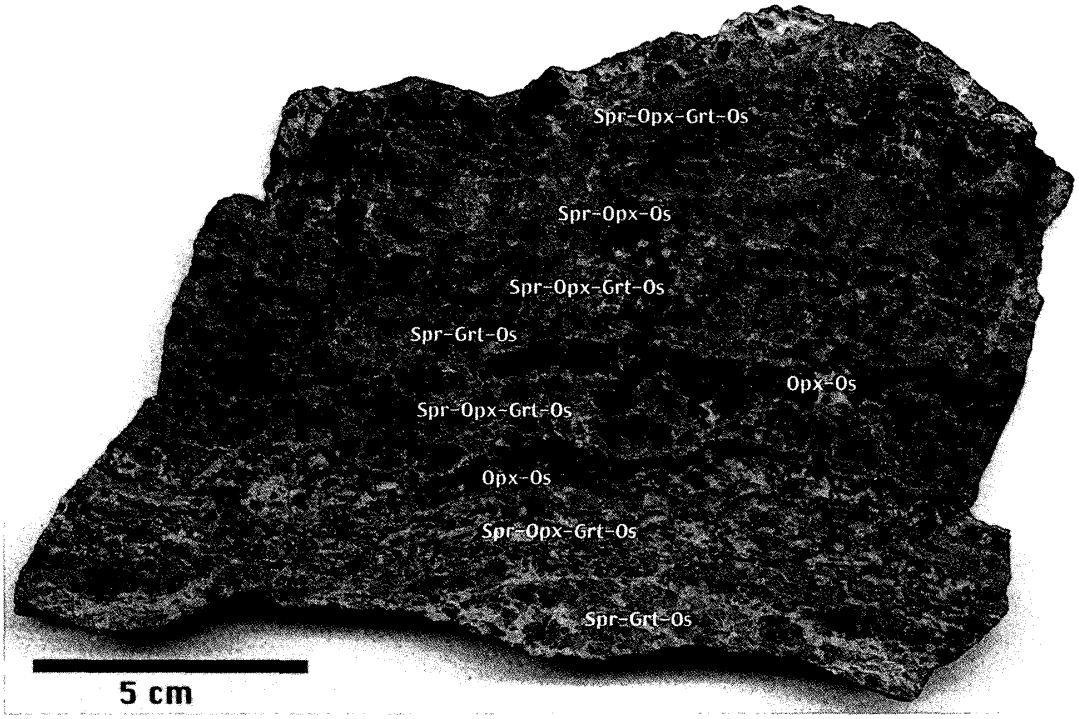

Fig. 5. Slab photo of banded osumilite-bearing aluminous granulite.

(1) Osumilite-bearing aluminous sapphirine granulite characteristically crops out between boudinaged ultramafic granulite and sillimanite-garnet-sapphirine gneiss, which in turn is surrounded by garnet- or orthopyroxene-bearing quartzofeldspathic gneisses (Fig. 4a). This rock is a dark colored massive granulite (Fig. 4b) and has a thickness ranging from several centimeters to several meters. Osumilite in this type of rock shows brilliant moon stone-like reflections in hand specimens (Fig. 4c). Thin layering with complicated assemblages is observed in granulite (Fig. 5).

(2) Quartz-dominant sapphirine-garnet-orthopyroxene gneiss, which is pale brown to gray, occurs as thin intercalation within garnet- or orthopyroxene-bearing quartzofeldspathic layered gneisses (Fig. 4d). There is a thin alternation of garnet-rich and garnet-poor parts (Fig. 4e). This gneiss contains huge porphyroblastic garnet (up to 10 cm in diameter), which is surrounded by symplectite of grayish "milky" quartz and sapphirine (Fig. 4f).

3. Petrography and reaction textures

The rocks described here include osumilite-bearing aluminous sapphirine granulite and quartz-predominant sapphirine-garnet-orthopyroxene gneiss, which indicate two modes of occurrence as mentioned above. Representative mineral chemical compositions of each rock type are shown in Table 1.

3.1. Osumilite-bearing aluminous sapphirine granulite

Osumilite-bearing aluminous granulites show medium- to coarse-grained massive texture and coexist with other UHT-type of metamorphic rocks at the boundary between metamorphosed ultramafic rocks (spinel-bearing orthopyroxenite and phlogopite-bearing orthopyroxenite) and garnet-bearing quartzofeldspathic granulite. Osumilite-bearing aluminous granulites are subdivided into the following three types of mineral assemblages:

(1) sapphirine + garnet + osumilite + quartz,
(2) sapphirine + orthopyroxene + garnet + osumilite ± quartz,
(3) orthopyroxene + osumilite ± sapphirine ± sillimanite ± quartz.

All these assemblages also contain K-feldspar and cordierite with subordinate spinel, phlogopite and plagioclase. Rare secondary biotite and gedrite are also present. Trace and accessory minerals are rutile, zircon and ilmenite with rare monazite, magnetite and srilankite. Srilankite is a rare mineral, which coexists with rutile. Corroded anhedral grains of sillimanite are included in sapphirine. Orthopyroxene and pale brownish quartz in these granulites have abundant acicular inclusions of rutile.

Some reaction textures in osumilite-bearing aluminous sapphirine granulite are shown in Fig. 6. In the orthopyroxene-free domain, garnet+sillimanite association is usually surrounded by sapphirine+quartz symplectite, where sapphirine includes sillimanite (Fig. 6a). Most osumilite coexists with garnet, sapphirine, K-feldspar and quartz (Fig. 6b), and is replaced by cordierite-bearing symplectite during the retrograde stage. Cordierite is also formed among garnet, sapphirine and quartz (Fig. 6c). Possible metamorphic reactions in the orthopyroxene-free domain are:

$$\text{garnet} + \text{sillimanite} = \text{sapphirine} + \text{quartz}, \qquad \text{(a)}$$

Table 1. Representative electron microprobe analyses of constituent minerals.

Sample No.	Osumilite-bearing sapphirine granulite											Sapphirine-quartz gneiss						
Anal. No.	7.1	7.12	2.49	2.51	1.1	5.21	5.30	5.6	5.29.5	2.4	2.5	35	14	2	8	2	17	21
	Opx core	Opx rim	Grt core	Grt rim	Spr	Os	Os	Crd	Bt	Pl	Kfs	Opx core	Opx rim	Grt core	Grt rim	Spr	Spl	Crd
SiO_2	49.20	51.50	40.13	40.39	14.30	61.34	61.74	51.17	40.72	61.51	65.31	48.30	49.80	40.57	39.24	16.20	0.00	51.21
TiO_2	0.10	0.10	0.00	0.22	0.33	0.12	0.01	0.15	3.65	0.00	0.00	0.30	0.00	0.00	0.10	0.10	0.04	0.20
Al_2O_3	11.60	7.40	22.26	22.42	59.62	22.95	22.43	33.53	13.56	23.88	18.40	11.00	7.80	23.01	21.52	56.50	56.97	32.90
Cr_2O_3	0.20	0.00	0.00	0.21	0.81	0.00	0.28	0.00	0.00	0.00	0.00	0.10	0.10	0.10	0.00	0.30	2.77	0.00
FeO	14.80	15.80	22.18	23.20	7.34	1.29	2.33	2.06	5.50	0.40	0.00	18.40	19.90	22.72	27.55	10.50	24.84	2.72
MnO	0.00	0.00	0.00	0.00	0.00	0.06	0.00	0.00	0.00	0.00	0.00	0.00	0.00	0.00	0.00	0.20	0.00	0.06
MgO	23.70	25.20	14.43	13.40	17.34	7.90	8.71	13.05	23.27	0.00	0.00	21.90	22.10	14.23	11.52	16.40	12.00	12.01
CaO	0.10	0.00	0.51	0.70	0.00	0.00	0.00	0.00	0.00	5.31	0.32	0.10	0.10	0.25	0.07	0.20	0.00	0.00
Na_2O	0.00	0.00	0.00	0.00	0.00	0.37	0.20	0.00	0.14	7.75	1.65	0.10	0.00	0.00	0.00	0.00	0.00	0.28
K_2O	0.00	0.00	0.00	0.00	0.00	4.09	4.05	0.00	9.94	2.12	13.53	0.00	0.10	0.00	0.00	0.00	0.00	0.00
ZnO	---	---	---	---	---	---	---	---	---	---	---	---	---	---	---	---	2.50	---
F	---	---	---	---	---	---	---	---	3.29	---	---	---	---	---	---	---	---	---
Cl	---	---	---	---	---	---	---	---	0.00	---	---	---	---	---	---	---	---	---
F=O	---	---	---	---	---	---	---	---	1.39	---	---	---	---	---	---	---	---	---
Cl=O	---	---	---	---	---	---	---	---	0.00	---	---	---	---	---	---	---	---	---
Total	99.70	100.00	99.51	100.54	99.74	98.12	99.75	99.96	98.68	100.97	99.21	100.20	99.90	100.88	100.00	100.40	99.12	99.38
O	6.000	6.000	12	12	10	30	30	18		8.00	8.00	6	6	12	12	10	4	18
Si	1.767	1.850	3.006	3.008	0.854	10.263	10.222	5.033	5.718	2.732	3.008	1.758	1.830	2.997	3.000	0.974	0.000	5.082
Ti	0.003	0.003	0.000	0.012	0.015	0.015	0.001	0.011	0.386	0.000	0.000	0.008	0.000	0.000	0.006	0.005	0.001	0.015
Al	0.491	0.313	1.965	1.968	4.197	4.526	4.377	3.887	2.244	1.250	0.999	0.472	0.338	2.004	1.939	4.002	1.858	3.848
Cr	0.006	0.000	0.000	0.012	0.038	0.000	0.037	0.000	0.000	0.000	0.000	0.003	0.003	0.006	0.000	0.014	0.061	0.000
Fe	0.444	0.475	1.389	1.445	0.367	0.181	0.323	0.169	0.646	0.015	0.000	0.560	0.612	1.404	1.761	0.528	0.575	0.226
Mn	0.000	0.000	0.000	0.000	0.000	0.009	0.000	0.000	0.000	0.000	0.000	0.000	0.000	0.000	0.000	0.010	0.000	0.005
Mg	1.268	1.349	1.611	1.487	1.543	1.970	2.149	1.913	4.872	0.000	0.000	1.188	1.210	1.567	1.313	1.469	0.495	1.776
Ca	0.004	0.000	0.041	0.056	0.000	0.000	0.000	0.000	0.000	0.253	0.016	0.004	0.004	0.020	0.006	0.013	0.000	0.000
Na	0.000	0.000	0.000	0.000	0.000	0.120	0.064	0.000	0.038	0.667	0.147	0.007	0.000	0.000	0.000	0.000	0.000	0.054
K	0.000	0.000	0.000	0.000	0.000	0.873	0.856	0.000	1.780	0.120	0.795	0.000	0.005	0.000	0.000	0.000	0.000	0.000
Zn	---	---	---	---	---	---	---	---	---	---	---	---	---	---	---	---	0.051	---
F	---	---	---	---	---	---	---	---	1.461	---	---	---	---	---	---	---	---	---
Cl	---	---	---	---	---	---	---	---	0.000	---	---	---	---	---	---	---	---	---
OH	---	---	---	---	---	---	---	---	2.539	---	---	---	---	---	---	---	---	---
XMg	0.741	0.740	0.537	0.507	0.808	0.916	0.869	0.919	0.883	---	---	0.680	0.664	0.527	0.427	0.736	0.463	0.887
XF									0.365									
Alm			0.452	0.484										0.469	0.564			
Sps			0.000	0.000										0.000	0.000			
Prp			0.535	0.498										0.524	0.434			
Grs			0.014	0.019										0.007	0.002			
An										0.243	0.016							
Ab										0.642	0.154							
Or										0.115	0.830							

garnet + sapphirine + K-feldspar + quartz = osumilite, (b)

sapphirine + K-feldspar + quartz = osumilite + sillimanite, (c)

garnet + sapphirine + quartz = cordierite. (d)

Representative photomicrographs of the orthopyroxene-bearing domain are shown in Figs. 6d, 6e and 6f. In this domain, sapphirine, garnet and orthopyroxene coexistence is commonly observed (Fig. 6d) and osumilite+garnet and osumilite+garnet+sillimanite

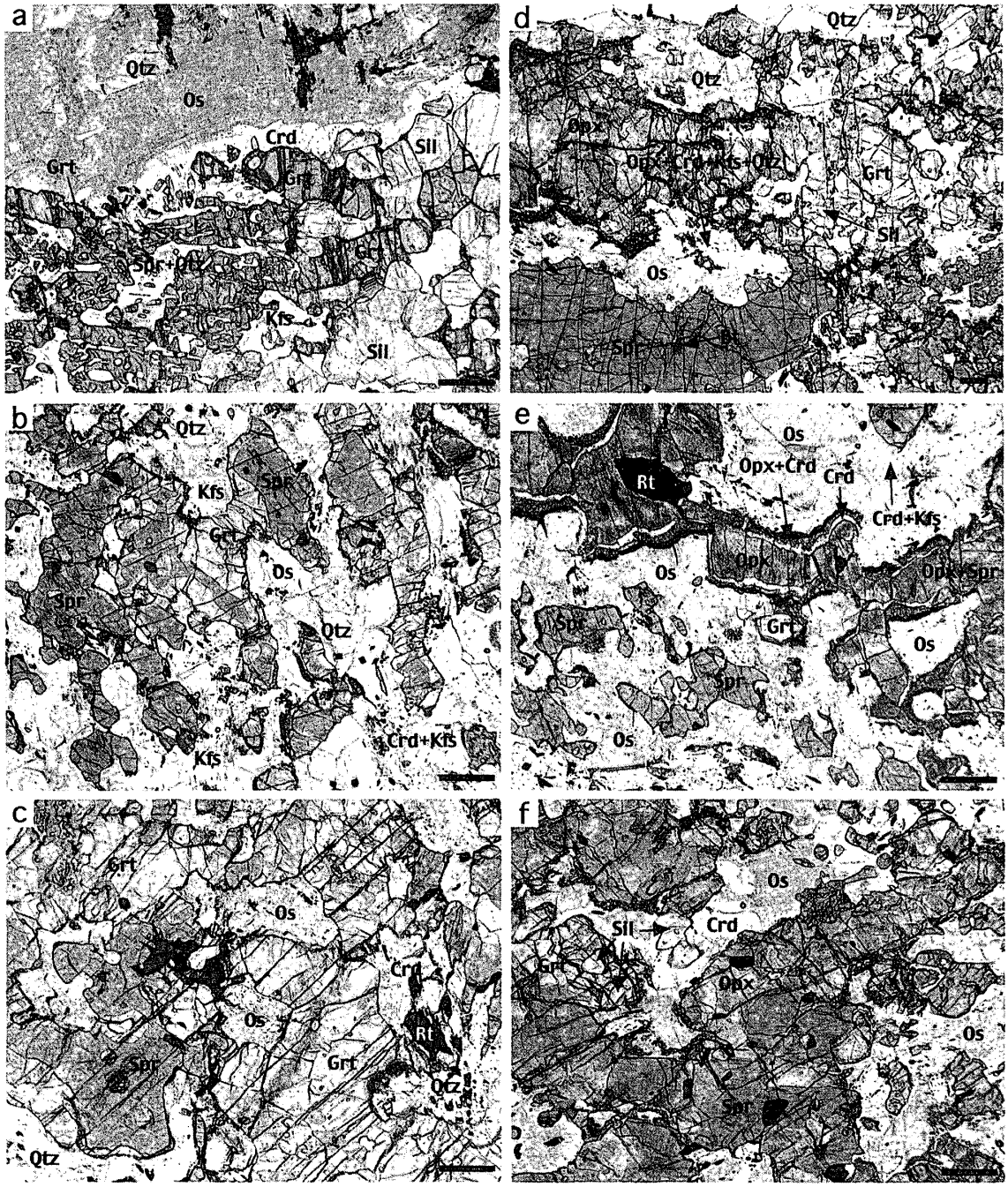

Fig. 6. Photomicrographs of osumilite-bearing aluminous granulite. a–c: sapphirine+garnet+osumilite+quartz association, d–f: sapphirine+orthopyroxene+garnet+osumilite±quartz association. Scale bar is 1 mm.

associations also occur (Figs. 6e and 6f). Complicated symplectitic intergrowth containing orthopyroxene, cordierite and K-feldspar also occurs at the boundary between orthopyroxene and osumilite (Figs. 6e and 7), where orthopyroxene+cordierite symplectite occurs next to porphyroblastic orthopyroxene, which is not shown in Fig. 7, and cordierite+ K-feldspar symplectite next to osumilite. A cordierite moat also occurs between porphyroblastic orthopyroxene and orthopyroxene+cordierite symplectite (Fig. 6e). These textures would indicate the following reactions during metamorphic evolution:

sapphirine + orthopyroxene + K-feldspar = garnet + osumilite, (e)

sapphirine + K-feldspar + quartz = garnet + sillimanite + osumilite, (f)

Al-rich orthopyroxene + osumilite =
Al-poor orthopyroxene + cordierite + K-feldspar, (g)

osumilite = orthopyroxene + cordierite + K-feldspar + quartz. (h)

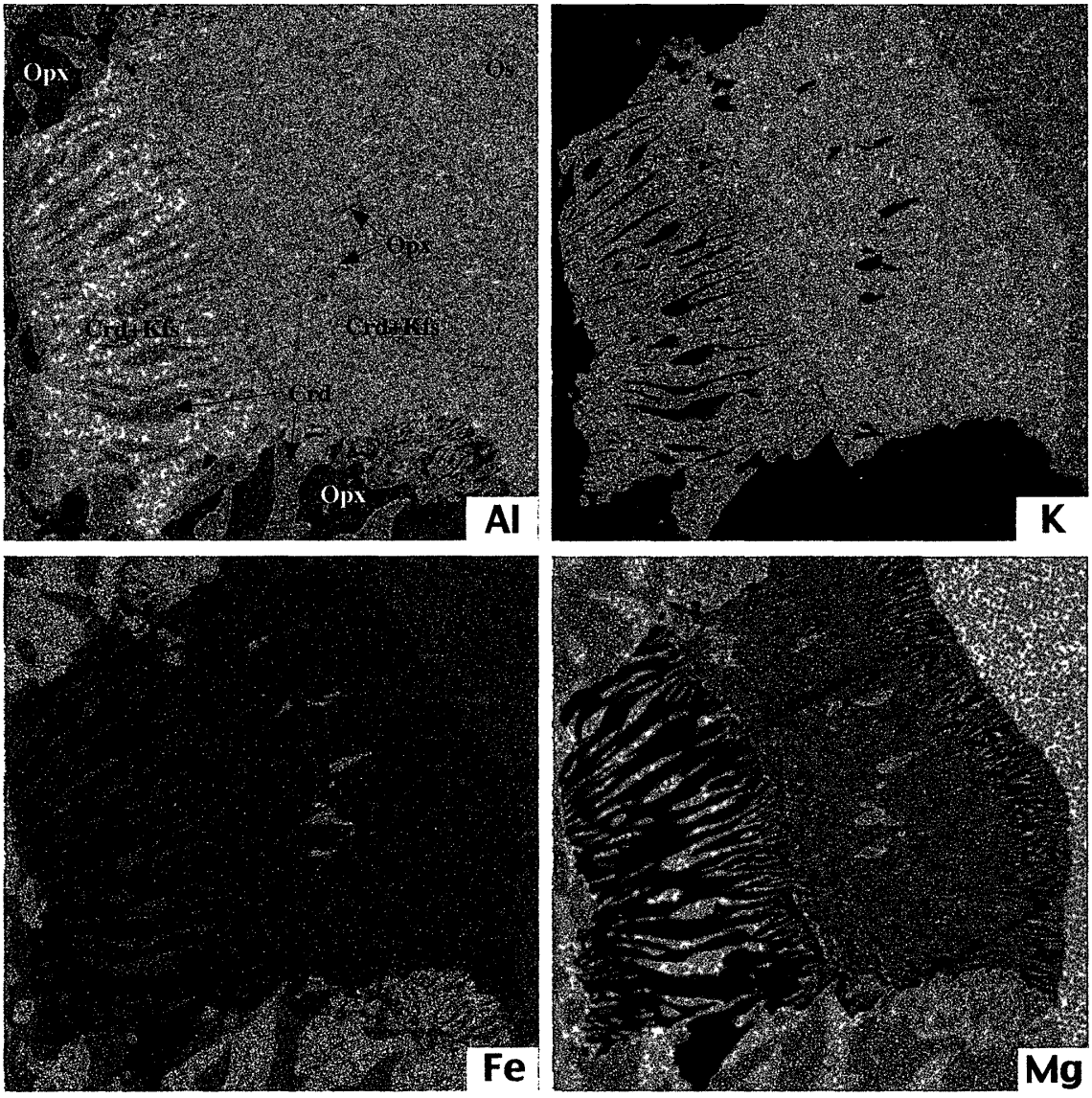

Fig. 7. EDS color mapping by element of symplectitic intergrowth among orthopyroxene, cordierite and K-feldspar at the boundary between orthopyroxene and osumilite.

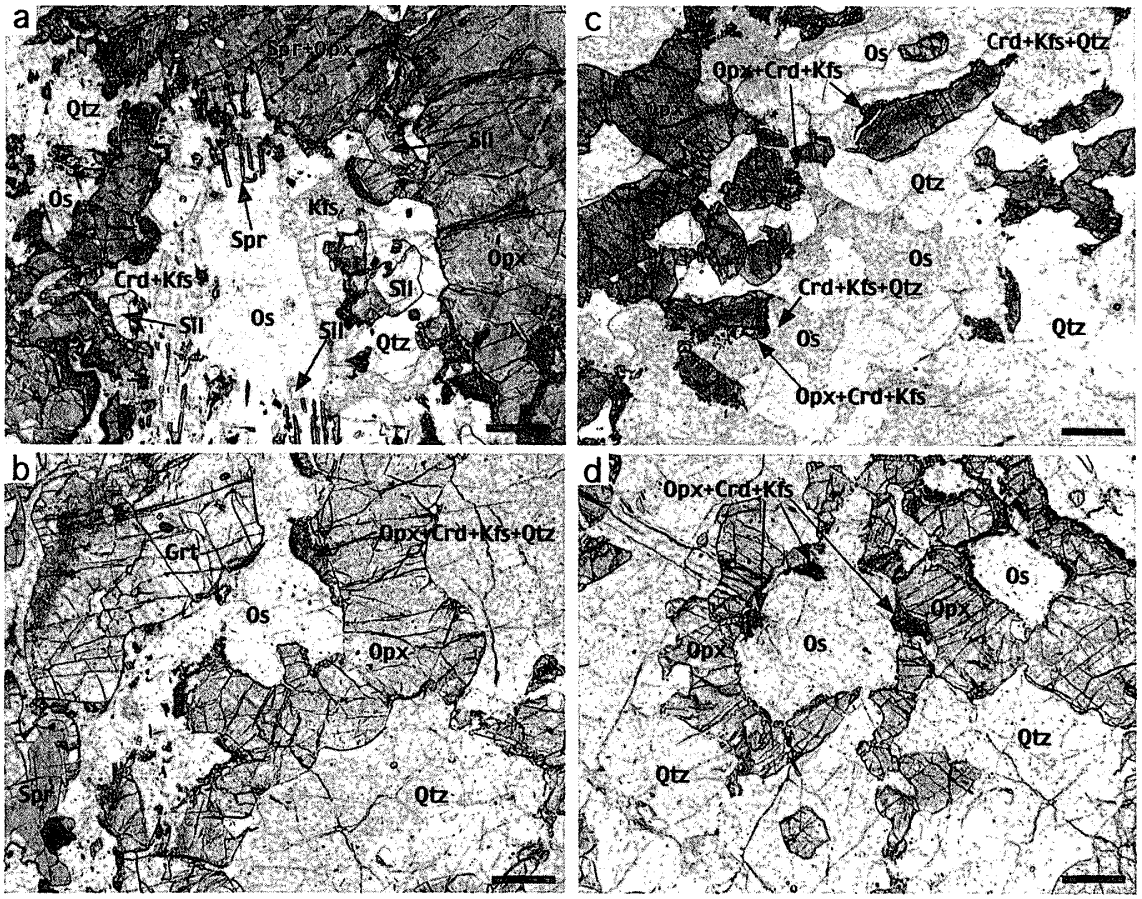

Fig. 8. Photomicrographs of garnet-poor or -free orthopyroxene-osumilite association. a–b: Sapphirine- and garnet-bearing portion, c–d: Sapphirine- and garnet-free portion. Scale bar indicates 1 mm.

Some more osumilite-forming reactions are also observed (Fig. 8). Figure 8a shows osumilite and sillimanite association formed by reaction (c). Osumilite and orthopyroxene also formed among garnet, quartz and K-feldspar (Fig. 8b). Garnet- and sapphirine-free orthopyroxene-osumilite domain consists mostly of orthopyroxene, osumilite and quartz (Figs. 8c, 8d). Orthopyroxene and quartz typically enclose very fine-grained rutile needles and show brownish color in the plane-polarized light. Symplectitic intergrowth containing cordierite, orthopyroxene and K-feldspar also occurs at the boundary between porphyroblastic orthopyroxene and osumilite as mentioned above. Other possible metamorphic reactions are as follows:

$$\text{garnet} + \text{K-feldspar} + \text{quartz} = \text{orthopyroxene} + \text{osumilite}. \qquad \text{(i)}$$

3.2. Sapphirine-quartz gneiss

Quartz-dominant sapphirine-garnet-orthopyroxene gneiss consists largely of sapphirine, garnet, orthopyroxene, sillimanite and quartz with subordinate meso-perthitic K-feldspar, spinel and cordierite. Accessories are ilmenite, rutile, zircon, monazite and apatite. The gneiss is subdivided into the following two types of mineral assemblages as thin layers or elongated micro domains:

(1) orthopyroxene + garnet + sapphirine + sillimanite + quartz,

(2) garnet + sapphirine + sillimanite + cordierite + spinel + quartz.

In the type-(1) assemblage, which is characterized by appearance of orthopyroxene and lack of spinel, garnet+orthopyroxene+sapphirine+quartz coexist and orthopyroxene+sillimanite is commonly surrounded by a garnet+sapphirine+quartz intergrowth (Figs. 9a 9b, 9c). Sapphirine includes anhedral orthopyroxene, sillimanite and quartz. These are microscopic evidence of the reactions:

orthopyroxene + sillimanite = garnet + sapphirine + quartz. (j)

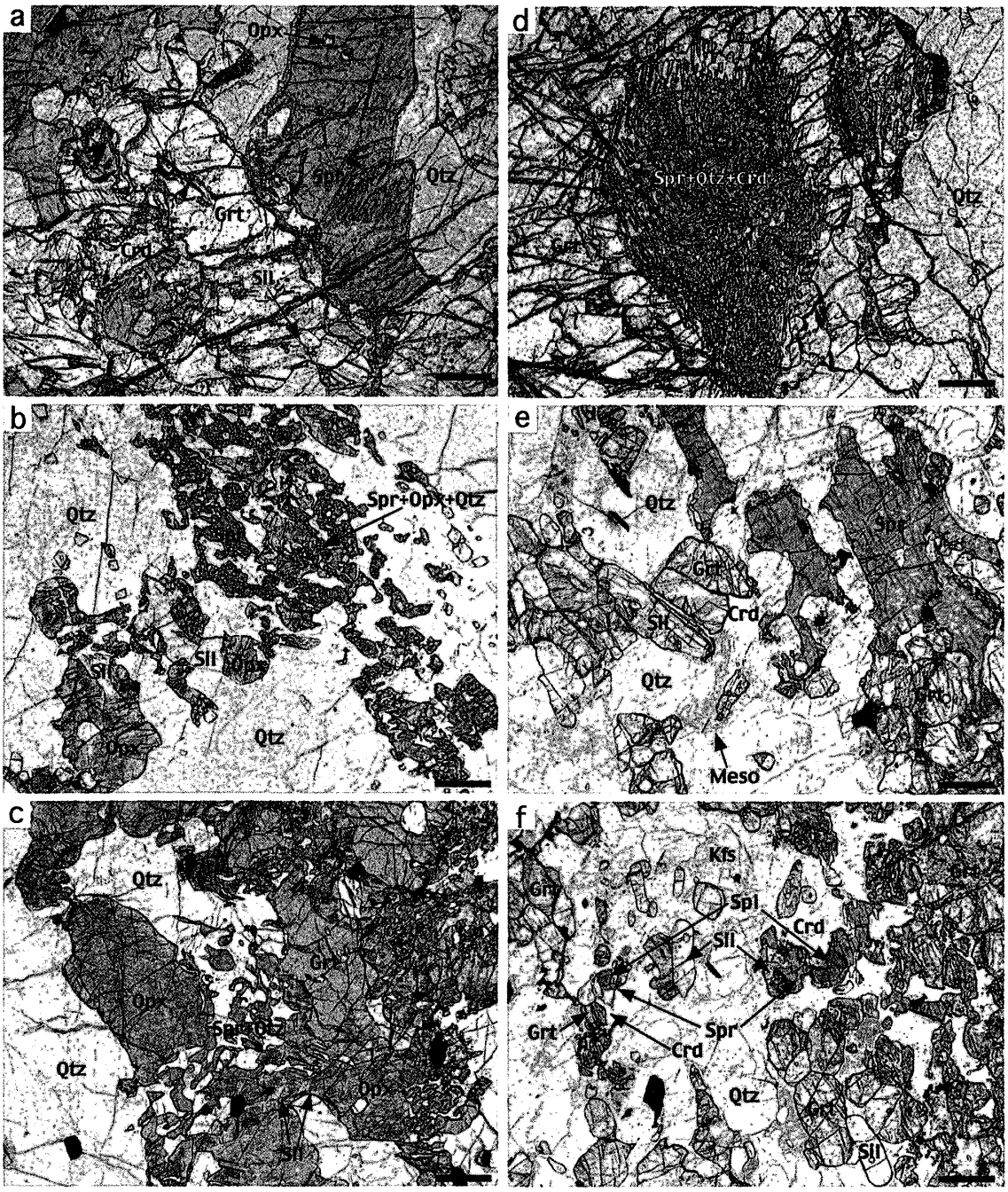

Fig. 9. Photomicrographs of quartz-dominant sapphirine-garnet-orthopyroxene gneiss. a–c: orthopyroxene-bearing portion, d–f: orthopyroxene-free portion. Scale bar is 1 mm.

The domain containing type-(2) assemblage in the sapphirine-quartz gneiss is characterized by presence of cordierite and predominance of sillimanite, whereas orthopyroxene was not found (Figs. 9d, 9e, 9f). Garnet, cordierite, sapphirine and quartz coexist can be observed (Figs. 9d and 10) and occasionally garnet, cordierite and sillimanite association also occurs (Fig. 9e). Spinel and cordierite coexistence occurs at the boundary among garnet, sapphirine and sillimanite. These textures would be interpreted to have formed during the retrograde metamorphic evolution through the following reactions:

sapphirine + orthopyroxene + quartz = garnet + cordierite, (k)

sapphirine + quartz = garnet + cordierite + sillimanite, (l)

garnet + sapphirine + sillimanite = cordierite + spinel. (m)

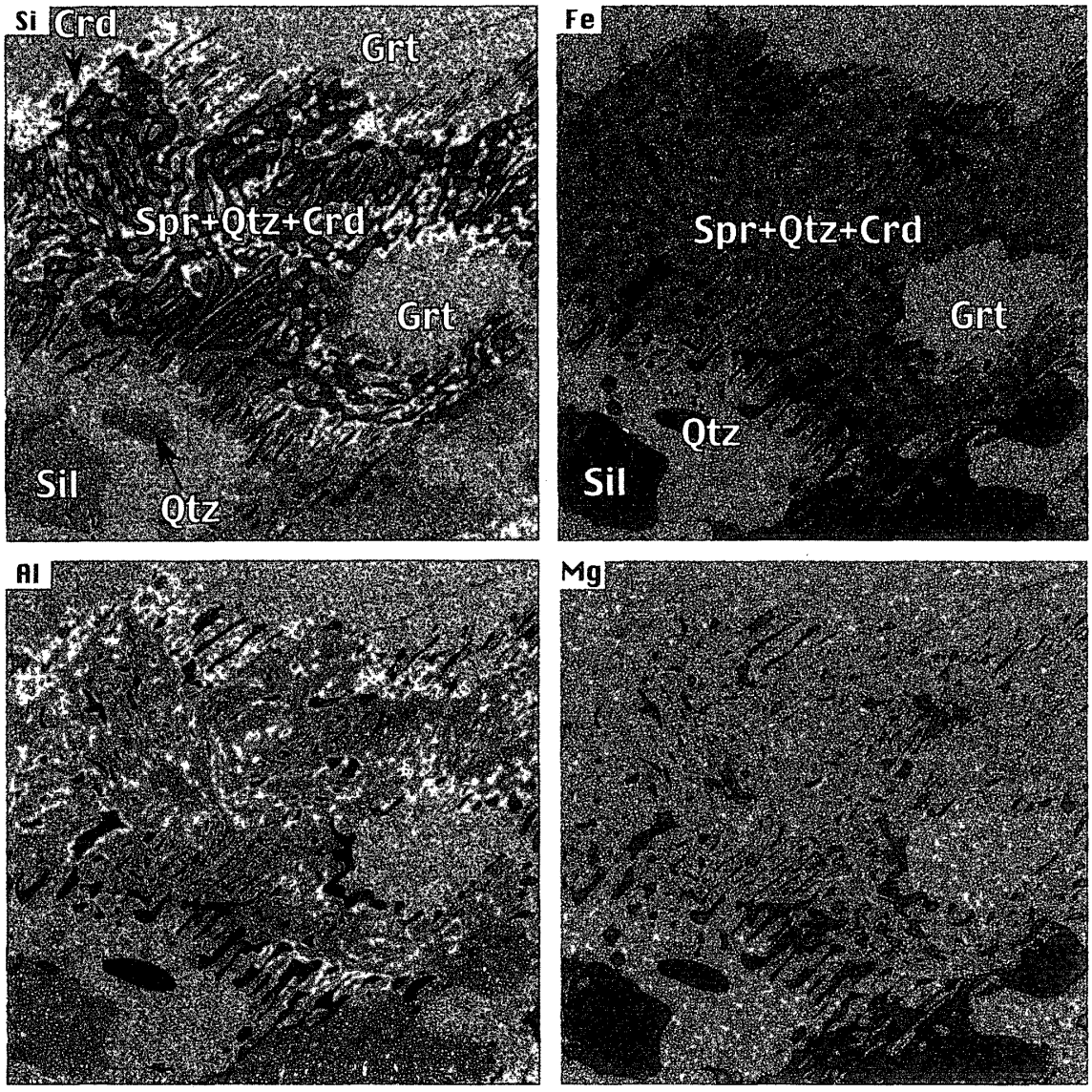

Fig. 10. EDS color mapping of sapphirine-quartz symplectite in garnet. Cordierite occurs as retrograde phase.

4. Whole rock chemistry

Major and trace element contents of osumilite-bearing aluminous granulites (103A, 103B) and sapphirine+quartz-bearing quartzofeldspathic gneisses (sapphirine-quartz gneiss: 207A, 208A, 208C), were determined by X-ray fluorescence spectrometry (Rigaku: RIX-2100) at Kurashiki University of Arts and Sciences. Volatiles were

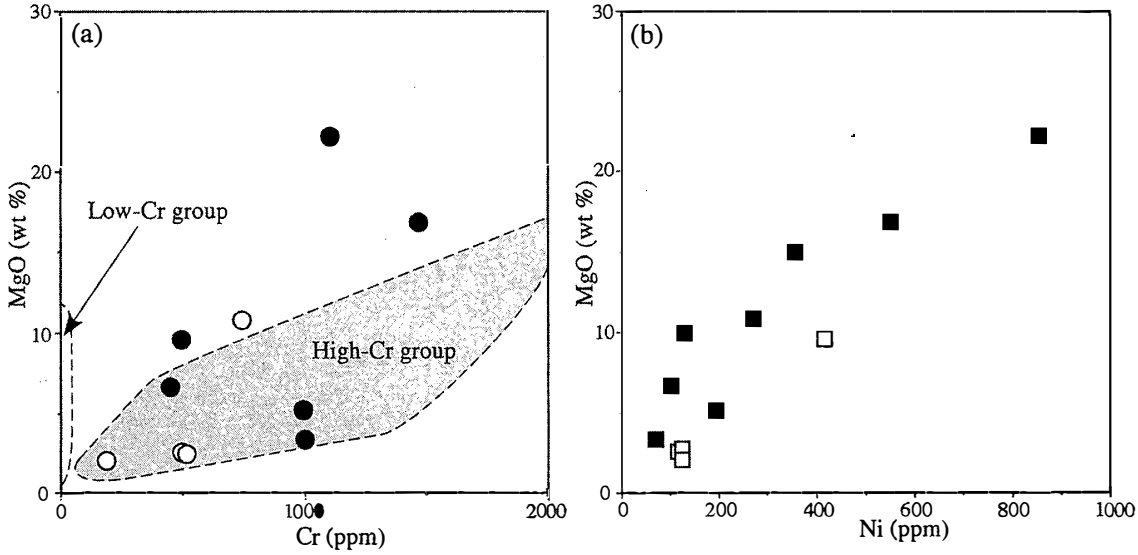

Fig. 11. Bulk chemical compositions of osumilite-bearing granulite and sapphirine-quartz gneiss from Bunt Island. (a) plot of MgO against Cr, (b) plot of MgO against Ni.

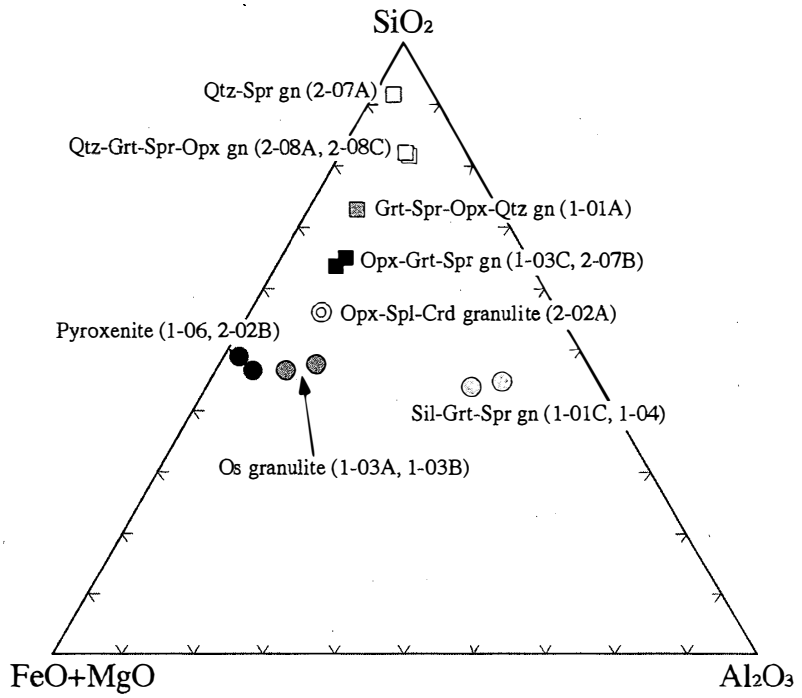

Fig. 12. SiO_2-Al_2O_3-(FeO+MgO) diagram showing bulk chemical compositions of osumilite-bearing granulite, sapphirine-quartz gneiss and related metamorphic rocks.

Table 2. Representative bulk chemical compositions and CIPW norm of UHT granulites from Bunt Island.

	01-01A	01-01C	01-03A	01-03B	01-03C	01-04	01-06	02-02A	02-02B	02-07A	02-07B	02-08A	02-08C
	Grt-Qtz gn	Sil-Grt-Spr gn	Os granulite	Os granulite	Opx-Grt-Spr gn	Sil-Grt-Spr gn	Orthopyroxenite	Opx-Spl-Crd gn	Orthopyroxenite	Qtz-Grt-Spr gn	Opx-Grt-Spr gn	Qtz-Grt-Spr gn	Qtz-Grt-Spr gn
SiO_2	70.67	34.56	44.71	43.62	62.07	34.70	48.09	46.47	51.38	90.25	61.25	74.15	73.68
TiO_2	0.51	1.61	1.29	1.42	0.77	1.50	1.52	0.28	0.26	0.18	1.14	0.72	0.68
Al_2O_3	10.90	53.76	16.63	21.79	15.27	50.17	8.23	14.23	3.09	4.40	13.99	14.02	14.92
FeO	10.33	5.01	15.83	17.17	9.00	6.49	20.90	8.02	21.14	2.75	13.52	4.10	4.04
MnO	0.14	0.05	0.06	0.06	0.05	0.05	0.23	0.19	0.54	0.03	0.10	0.04	0.04
MgO	6.68	4.38	19.11	13.80	10.80	6.13	20.55	13.41	21.26	2.04	9.55	2.63	2.55
CaO	0.64	0.31	0.26	0.35	0.33	0.31	0.30	17.13	2.10	0.17	0.39	0.61	0.53
Na_2O	0.10	0.19	0.29	0.39	0.40	0.24	0.09	0.16	0.09	0.06	0.04	0.78	0.69
K_2O	0.00	0.11	1.43	1.00	1.32	0.40	0.07	0.02	0.01	0.11	0.01	1.93	1.86
P_2O_5	0.02	0.01	0.01	0.01	0.01	0.01	0.01	0.09	0.13	0.01	0.01	0.01	0.01
Ig. loss	0.15	0.18	0.40	0.21	0.32	0.25	0.27	0.57	0.31	0.46	0.63	0.77	1.04
Ba	31.7	59.2	350.6	248.0	152.0	185.0	32.7	7.6	12.6	64.5	149.0	634.5	739.8
Co	0.0	0.0	0.0	0.0	0.0	0.0	0.0	0.0	0.0	0.0	0.0	0.0	0.0
Cr	443.2	1003.0	1104.0	1467.7	744.7	997.6	1370.2	1696.7	1352.8	191.4	500.4	501.2	512.0
Ga	0.0	0.0	0.0	0.0	0.0	0.0	0.0	0.0	0.0	0.0	0.0	0.0	0.0
Hf	0.0	0.0	0.0	0.0	0.0	0.0	0.0	0.0	0.0	0.0	0.0	0.0	0.0
Nb	25.7	19.0	11.2	34.4	14.1	15.5	17.6	4.0	0.8	2.1	9.0	9.7	10.6
Ni	100.2	68.9	858.8	548.9	271.9	194.2	460.0	654.8	429.9	123.3	411.2	118.8	116.1
Rb	1.2	1.1	61.2	15.4	14.1	4.9	1.1	2.5	0.4	1.8	1.4	28.8	27.1
Sr	0.4	5.8	4.7	3.2	2.8	7.8	1.7	36.2	5.5	0.2	1.7	56.0	54.9
V	108.1	485.8	248.9	397.5	183.2	428.7	375.7	68.6	112.6	32.8	187.0	119.5	123.7
Y	47.5	21.2	12.9	18.5	14.5	17.8	37.4	7.1	6.3	3.2	24.1	14.0	14.3
Zn	36.0	33.1	129.5	95.9	63.6	51.6	152.2	503.8	205.8	15.6	42.4	32.4	33.6
Zr	253.4	270.2	290.7	465.8	273.7	254.7	991.0	47.1	10.9	214.2	362.1	386.0	351.9
F	50.0	50.0	2200.0	80.0	50.0	40.0	50.0	150.0	110.0	40.0	40.0	40.0	40.0
A.S.I.	8.19	51.64	6.66	9.27	5.68	35.03	10.24	0.45	0.78	8.22	17.76	3.13	3.63
XMg	0.54	0.50	0.78	0.70	0.68	0.55	0.61	0.75	0.64	0.57	0.56	0.53	0.53
CIPW norm													
Q	50.44	22.86		2.91	30.93	17.68				83.88	35.39	56.04	55.32
C	9.62	52.80	14.21	19.53	12.59	48.81	7.49			3.88	13.22	10.09	10.95
or		0.65	8.47	5.92	7.79	2.36	0.41	0.11	0.09	0.65	0.08	11.12	11.07
ab	0.86	1.59	2.46	3.30	3.39	2.01	0.76	1.33	0.73	0.53	0.35	5.92	5.90
an	3.03	1.45	1.24	1.68	1.60	1.46	1.43	38.07	7.99	0.81	1.87	2.59	2.58
di								37.39	1.30				
wo								19.35	0.66				
en								12.55	0.37				
fs								5.49	0.27				
hy	35.01	17.55	61.02	63.93	42.23	24.81	85.71	2.51	82.00	9.89	46.92	12.84	12.84
en	16.64	10.92	38.91	34.51	26.89	15.26	50.15	1.75	47.02	5.08	23.78	6.44	6.41
fs	18.38	6.63	22.11	29.42	15.34	9.55	35.56	0.76	34.98	4.82	23.13	6.40	6.43
ol			10.12				1.29	19.84	7.10				
fo			6.23				0.72	13.39	3.90				
fa			3.90				0.57	6.45	3.20				
il	0.98	3.06	2.45	2.71	1.46	2.85	2.89	0.54	0.49	0.34	2.16	1.38	1.31
ap	0.05	0.02	0.02	0.02	0.01	0.02	0.02	0.21	0.30	0.02	0.02	0.03	0.03

A.S.I. (alumina saturation index)=$Al_2O_3/(CaO+Na_2O+K_2O)$.

determined by loss on ignition. Representative data of the major and trace elements with calculated C.I.P.W. norms for osumilite-bearing granulites, sapphirine-quartz gneisses and other metamorphic rocks are presented in Table 2.

Osumilite-bearing granulite is characterized by high Al_2O_3, MgO, K_2O, Cr, Ni, Ba, Rb and Zn. The highest Mg# (=Mg/Fe+Mg: 0.68–0.76) values are recognized for osumilite-bearing granulite. Contiguous quartz-free sillimanite-garnet-sapphirine gneisses (101C, 104) are extremely high in Al_2O_3 and low in SiO_2 with relatively low Mg# (0.47–0.52). These hyper-aluminous, nearly silica-undersaturated bulk chemical compositions have significant normative corundum (47–52%) and in some cases normative olivine (Table 1). Almost all of the sapphirine-quartz gneisses intercalated within layered gneiss have high SiO_2, Ba, Rb, and Sr contents and show low FeO and MgO values with moderate Mg# (0.50–0.54). Sheraton (1980) divided high-grade

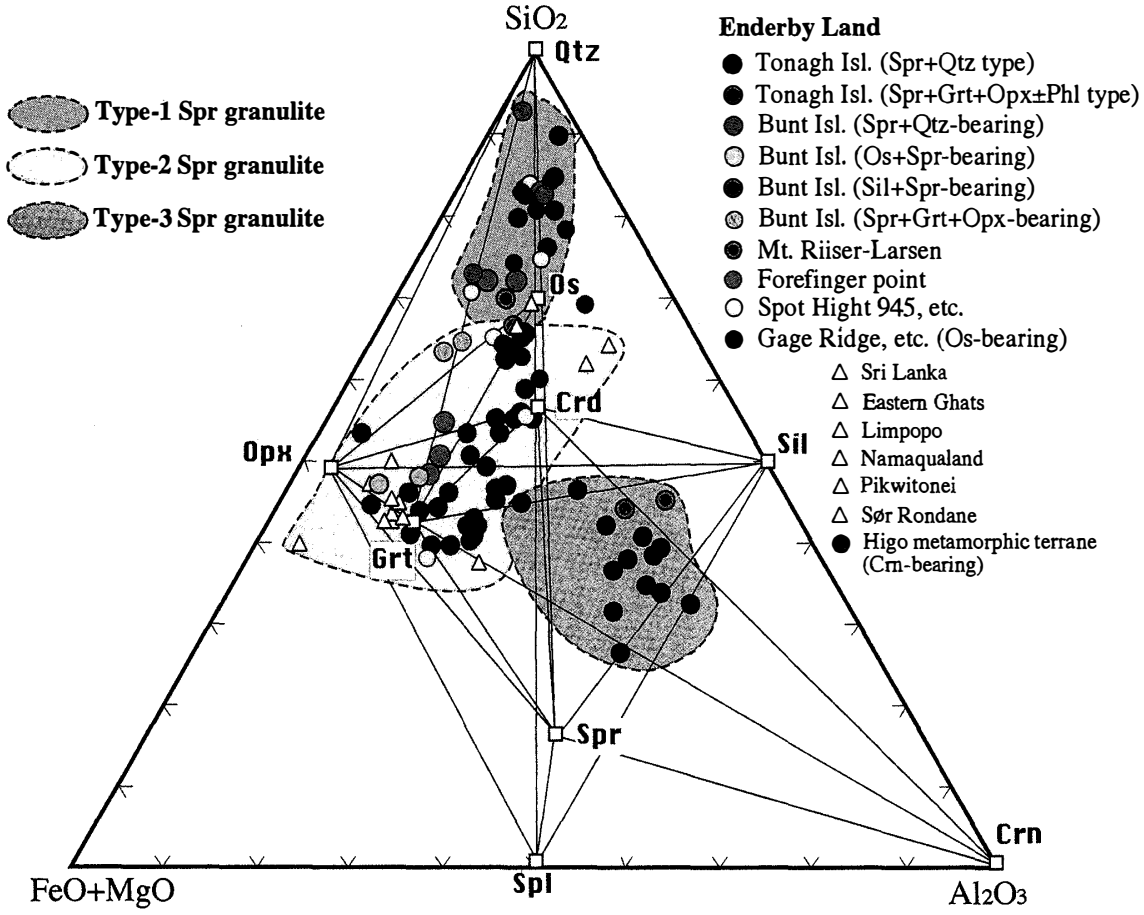

Fig. 13. Compiled sapphirine granulite compositions of the world plotted on the SiO_2-Al_2O_3-(FeO+MgO) diagram. Type-1: quartz-dominant sapphirine+quartz type, Type-2: quartz-poor or -free sapphirine-garnet-orthopyroxene type, Type-3: quartz-free sapphirine-corundum or sapphirine-sillimanite type.
Data sources are as follows: Forefinger point: Harley et al., 1990; Tonagh Island: Osanai et al., 2001; Mt. Riiser-Larsen: Suzuki et al., 1999 and Spot Hight 945 etc.: Sheraton et al., 1987; Gage ridge etc.: Grew, 1982; Eastern Ghats, India: Sengupta et al., 1991; Limpopo belt, South Africa: Horrocks, 1983; Pikwitonei, Canada: Arima and Barnett, 1984; Sør Rondane, Antarctica: Ishizuka et al., 1995; Highland Complex, Sri Lanka: Osanai et al., 1996; Namaqualand, South Africa: Clifford et al., 1981 and Higo terrane, Japan: Osanai et al., 1998.

metapelites from Napier Complex into Cr-poor and Cr-rich categories. The latter presumably reflects a high-proportion of mafic and ultramafic source materials in the sedimentary precursor. The UHT-metamorphic rocks investigated here show Sheraton's Cr-rich affinity (Fig. 11a). Good correlation between MgO and Ni also indicates a strong effect of a high-proportion of mafic and ultramafic materials (Fig. 11b).

Whole rock compositions of the osumilite-bearing granulite, sapphirine-quartz gneiss and related granulites have been plotted on SiO_2-(FeO+MgO)-Al_2O_3 (FMAS) diagrams (Figs. 12 and 13). Sapphirine-quartz gneisses and quartz-bearing garnet-sapphirine-orthopyroxene gneiss plot rather close to the SiO_2-apex and osumilite-bearing granulites plot close to orthopyroxenite and are situated on the joint between ultramafic granulite (orthopyroxenite) and hyper aluminous sillimanite-garnet-sapphirine gneisses (Fig. 12). In Fig. 13 the UHT-metamorphic rocks from Bunt Island are compared with those of other sapphirine-bearing granulites from other areas of the Napier Complex. According to Osanai *et al.* (1999) sapphirine-bearing granulites are subdivided into three-types: (1) sapphirine-quartz coexisting type, (2) quartz-poor or -free sapphirine-orthopyroxene type, and (3) hyper aluminous corundum-sapphirine and sillimanite-sapphirine type. Sapphirine granulites from Bunt Island plot within the fields of all three types (Fig. 13). Almost all the sapphirine granulites from Tonagh Island have aluminous affinity with high-ASI (alumina saturation index) values up to 11.0, while those from Bunt Island are hyper aluminous with ASI up to 51.6 in sillimanite-predominant garnet-sapphirine gneiss (Fig. 14).

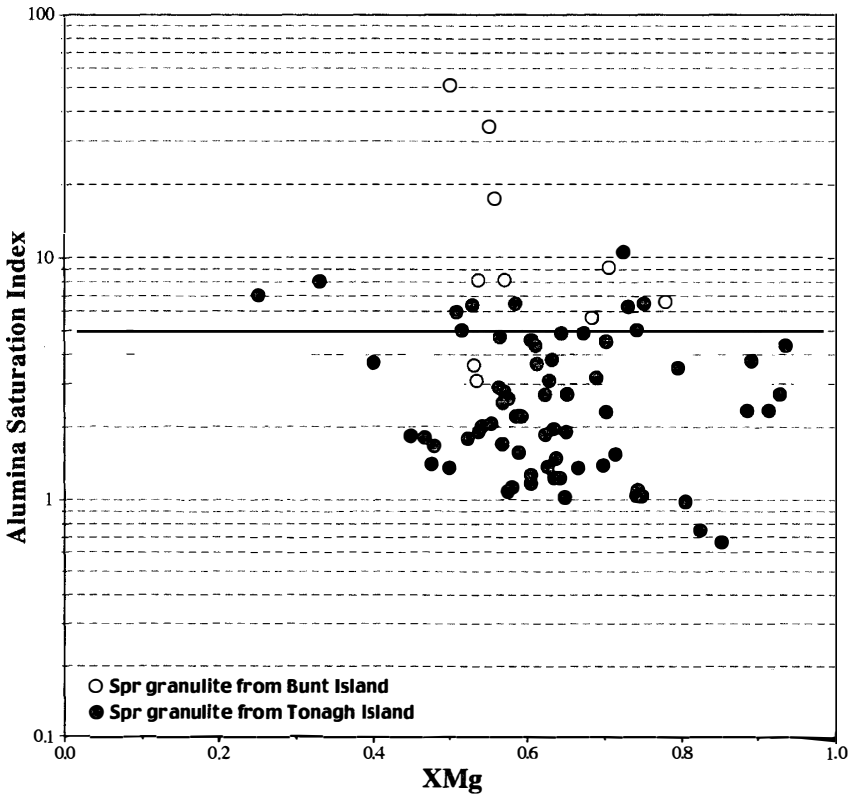

Fig. 14. XMg vs. A.S.I. (alumina saturation index) diagram. Aluminous granulites from Bunt Island have higher A.S.I. values than those from Tonagh Island.

5. *P-T* estimation for peak metamorphic condition

The mineral reactions observed in the osumilite-bearing aluminous granulites can be interpreted in the five-component (KFMAS) and seven-phase (Grt, Os, Opx, Spr, Crd, Kfs and Qtz) system. Hensen and Motoyoshi (1992) presented the schematic KFMAS petrogenetic grid to explain the osumilite and sapphirine stability (Fig. 15). When we try to use this grid, mineral reaction textures described above indicate a clockwise *P-T* evolution with isothermal decompression, but the reliable *P-T* condition is not realized yet. The grid used here is calculated by the THERMOCALC program including their thermodynamic data set (Holland and Powell, 1998) and natural chemical compositions of each mineral from osumilite-bearing aluminous granulites. Chemical compositions of each mineral for calculation are shown in Table 3. Calculated possible stable intersections are shown in Fig. 16 and their related reaction equations are listed in Table 4. On the basis of the petrographic observations described above, the divariant mineral assemblage garnet+sillimanite+K-feldspar was replaced by sapphirine+garnet+K-feldspar through the reaction of equation (a) and then sapphirine+garnet+osumilite produced by reaction (b). These sapphirine-consuming and osumilite-producing reactions took place at higher temperature condition beyond the invariant points [Crd, Opx] and [Os, Opx, Kfs] by an isothermal decompression process. This petrogenetic grid indicates that sapphirine+osumilite would be stabilized at temperature >1034°C and pressure <980 MPa, and the peak *P-T* condition (sapphirine+garnet+K-feldspar+quartz) is nearly the same as on Tonagh Island (T<1100°C, P<1100 MPa: Hokada *et al.*, 1999). This

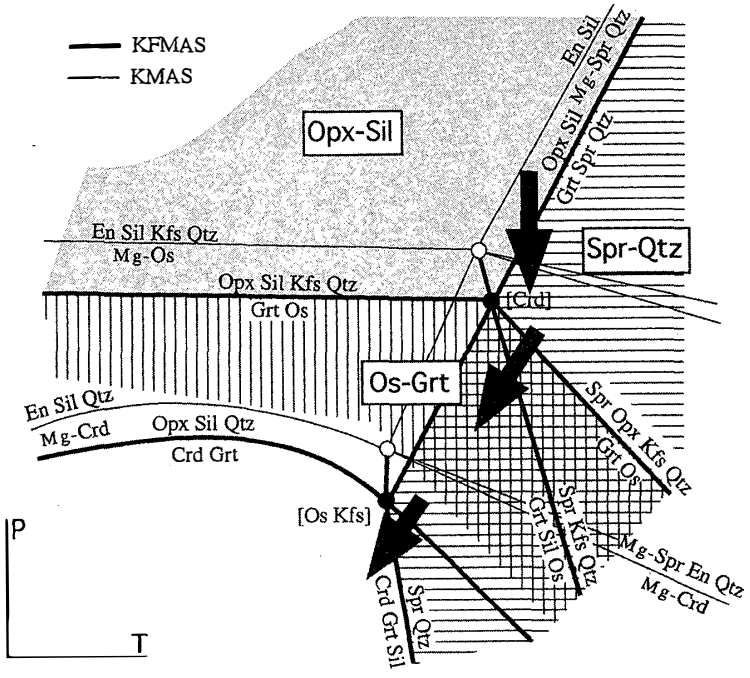

Fig. 15. Schematic pressure-temperature grid for KFMAS and KMAS system relevant to osumilite stability (modified after Hensen and Motoyoshi, 1992). Invariant points [Crd] and [Os, Kfs] are believed to be close to 1050°C and 1000–1100 MPa. Only reactions involving quartz are shown.

Table 3. Mineral compositions for calculation of petrogenetic grid.

Anal. No.	1-2-42	1-5-22	1-2-13	1-2-29	1-5-6	1-2-16
	Spr	Os	Grt	Opx	Crd	Kfs
SiO_2	14.65	60.83	40.46	48.93	51.17	65.05
TiO_2	0.07	0.57	0.24	0.11	0.15	0.00
Al_2O_3	60.63	23.31	22.88	10.43	33.53	18.76
Cr_2O_3	0.50	0.00	0.00	0.00	0.00	0.00
FeO	7.29	1.62	21.00	15.99	2.06	0.00
MnO	0.00	0.12	0.00	0.00	0.00	0.00
MgO	16.72	8.49	14.31	24.06	13.05	0.00
CaO	0.00	0.04	0.97	0.07	0.00	0.13
Na_2O	0.00	0.16	0.00	0.00	0.00	1.30
K_2O	0.00	4.15	0.00	0.00	0.00	13.91
Total	99.86	99.29	99.86	99.59	99.96	99.15
O	10	30	12	6	18	8
Si	0.871	10.100	3.003	1.771	5.033	2.999
Ti	0.003	0.071	0.013	0.003	0.011	0.000
Al	4.249	4.562	2.002	0.445	3.887	1.019
Cr	0.023	0.000	0.000	0.000	0.000	0.000
Fe	0.362	0.225	1.304	0.484	0.169	0.000
Mn	0.000	0.017	0.000	0.000	0.000	0.000
Mg	1.481	2.101	1.583	1.298	1.913	0.000
Ca	0.000	0.007	0.077	0.003	0.000	0.006
Na	0.000	0.052	0.000	0.000	0.000	0.116
K	0.000	0.879	0.000	0.000	0.000	0.818
XMg	0.804	0.903	0.548	0.728	0.919	

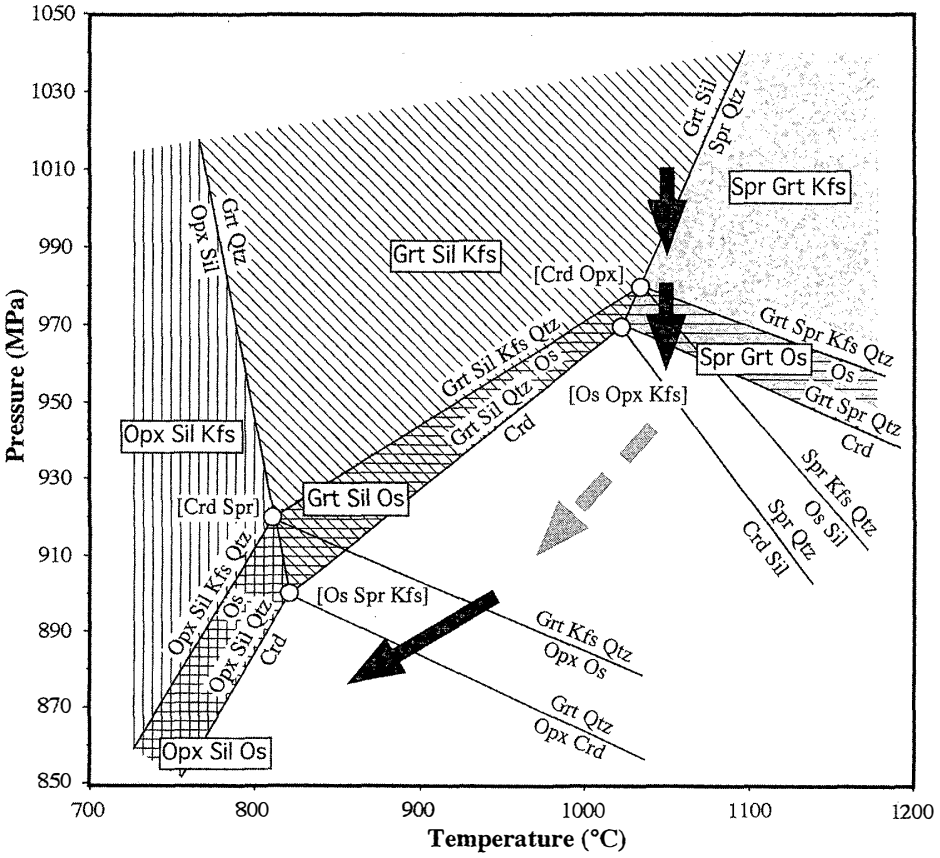

Fig. 16. Calculated pressure-temperature grid for KFMAS system using THERMOCALC program.

Table 4. Possible stable intersections and reaction equations.

Invariant [Crd Spr]		
2Sil + 3Opx = 2Grt + 2Qtz	(Os Kfs)	
2Grt + Kfs + 5Qtz = Os + 2Opx	(Sil)	Eq. (i)
2Grt + 4Sil + 3Kfs + 11Qtz = 3Os	(Opx)	
2Sil + Opx + Kfs + 3Qtz = Os	(Grt)	
Invariant [Os Spr Kfs]		
2Sil + 3Opx = 2Grt + 2Qtz	(Crd)	
Crd + 2Opx = 2Grt + 3Qtz	(Sil)	
3Crd = 2Grt + 4Sil + 5Qtz	(Opx)	
2Sil + Opx + Qtz = Crd	(Grt)	
Invariant [Os Opx Kfs]		
4Spr + 33Qtz = 4Sil + 7Crd	(Grt)	
Grt + 2Spr + 19Qtz = 5Crd	(Sil)	Eq. (d)
3Crd = 2Grt + 4Sil + 5Qtz	(Spr)	
6Spr + 32Qtz = 7Grt + 20 Sil	(Crd)	
Invariant [Crd Opx]		
4Spr + 7Kfs + 47Qtz = 7Os + 4Sil	(Grt)	Eq. (c)
Grt + 2Spr + 5Kfs + 29Qtz = 5Os	(Sil)	
2Grt + 4Sil + 3Kfs + 11Qtz = 3Os	(Spr)	Eq. (b)
6Spr + 32Qtz = 7Grt + 20Sil	(Os Kfs)	Eq. (a)

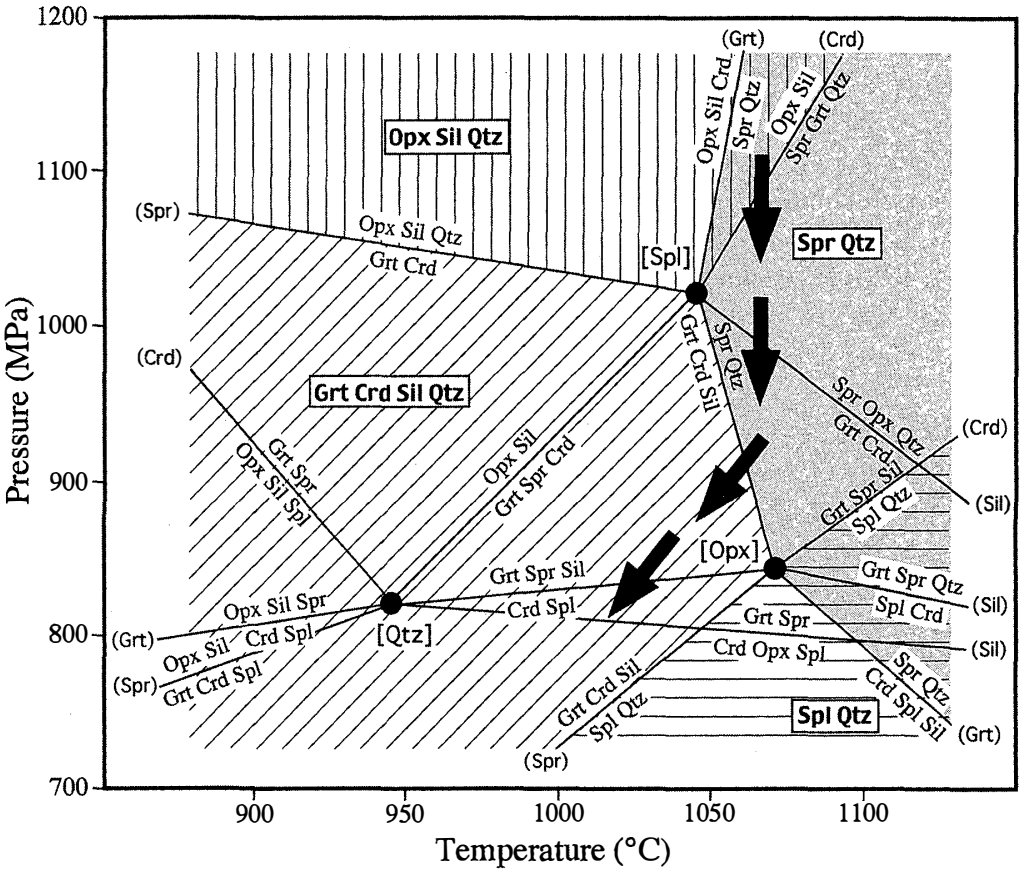

Fig. 17. Pressure-temperature diagram of the model FMAS system for explaining the metamorphic evolution of sapphirine-quartz gneiss under low-fO_2 condition (modified after Harley, 1998).

ultrahigh-temperature and relatively high-pressure condition is also supported by the appearance of aluminous orthopyroxene (up to 10.5 wt% Al_2O_3) and magnesian garnet (X_{Mg} up to 0.55).

Peak *P-T* estimation during metamorphic evolution for the sapphirine-quartz gneiss is explained using FMAS petrogenetic grid by Harley (1998) (Fig. 17). Observed mineral reaction textures described above show possible sequential isothermal decompression and near isobaric cooling processes from the orthopyroxene+ sillimanite+quartz field to the garnet+cordierite+sillimanite+quartz field through the sapphirine+quartz field. The primary orthopyroxene+sillimanite+quartz association gives the minimum pressure condition (*c.* 1020 MPa<*P*) and subsequent sapphirine+ quartz is stabilized in higher temperature condition than *c.* 1050°C (beyond [Spl] invariant point). Therefore the considered peak *P-T* condition for the sapphirine-quartz gneiss is similar to that of osumilite-bearing aluminous granulite. Aluminous orthopyroxene (Al_2O_3 =11.0 wt% and X_{Mg}=0.68) and magnesian garnet (X_{Mg}=0.54) in sapphirine-quartz gneiss indicate *c.* 1100°C and *c.* 1000 MPa, equivalent to stability of sapphirine+garnet+orthopyroxene+quartz, using X_{Mg} and X_{Al} isopleth diagram for garnet and orthopyroxene (Hensen and Harley, 1990; Aranovich and Berman, 1996).

6. Discussion and conclusions

6.1. Origin of osumilite-bearing granulite

Osumilite-bearing aluminous granulite is situated as a thin band between ultramafic granulite (garnet-bearing orthopyroxenite) and hyper aluminous sillimanite-garnet-sapphirine gneiss. The bulk chemical compositions of osumilite-bearing granulite are characterized by high Al_2O_3 (*c.* 20 wt%), MgO (*c.* 20 wt%) and K_2O (*c.* 1.2 wt%) with silica-undersaturated affinity (non or little normative quartz). Origins proposed for these silica-undersaturated aluminous ultrahigh-temperature metamorphic rocks were reviewed by many workers as well as Sheraton (1980), Droop and Bucher-Nurminen (1984), Arima and Barnett (1984), Pattison and Tracy (1991) and Osanai *et al.* (1998), and include:

(1) isochemical metamorphism of unusual sedimentary bulk compositions,
(2) metamorphism of hydrothermally altered basalts,
(3) metamorphism of ultramafic rocks (troctolitic composition),
(4) restite remaining after partial melting of pelitic rocks,
(5) high-grade contact metamorphism and/or metasomatism.

However, rock classification using protoliths is difficult for ultrahigh-temperature metamorphic rocks, especially in rocks having extreme chemical compositions. Sheraton (1980) suggested that the Cr-rich metapelites from the Napier Complex could be metamorphosed sediments containing high proportions of detritus from mafic to ultramafic rocks. The whole rock chemistry of osumilite-bearing aluminous granulite from Bunt Island also indicates Cr-rich affinity, equivalent to Sheraton's category. Owada *et al.* (1994) and Osanai *et al.* (2001) reported that the emplacement age for komatiitic basalt as a protolith of mafic to ultramafic granulite in the Napier Complex was *c.* 3.7 Ga. Zircon ages from felsic orthogneiss in the Amundsen Bay region of the Napier Complex by SHRIMP method are *c.* 3.2 Ga for core (emplacement age) and *c.* 2.5 Ga for

rim (metamorphic age) (Shiraishi *et al.*, 1997). The most effective UHT-metamorphic event would have taken place at *c.* 2.5 Ga (*e.g.* Owada *et al.*, 1994; Asami *et al.*, 1998). Therefore the mixing of clayey materials or other felsic components derived from felsic igneous rocks with a relatively high proportion of mafic to ultramafic detritus in the sedimentary precursor could have occurred during *c.* 3.2 and *c.* 2.5 Ga.

6.2. Metamorphic evolution of UHT-metamorphic rocks

Osumilite is one of the most important minerals for understanding ultrahigh-temperature metamorphism. During the past two decades, many experimental and theoretical studies on osumilite stability at ultrahigh-temperatures have been published (*e.g.* Ellis *et al.*, 1980; Grew, 1982; Motoyoshi *et al.*, 1993; Audibert *et al.*, 1993; Carrington and Harley, 1995; Holland *et al.*, 1996). These papers reported petrogenetic grids involving osumilite, garnet, orthopyroxene, cordierite, sillimanite, biotite, K-feldspar and quartz, but not sapphirine. As described above, ultrahigh-temperature osumilite-bearing aluminous granulite from Bunt Island contains not only sapphirine-free assemblage but also sapphirine+osumilite coexistence. Therefore we developed a sapphirine- and osumilite-bearing petrogenetic grid to show the metamorphic evolution of osumilite-bearing granulite from Bunt Island (Fig. 16). Metamorphic evolution at around the peak metamorphic condition is explained above, this was followed by sapphirine-, garnet- and orthopyroxene-consuming and osumilite- and cordierite-producing reactions during the retrograde metamorphic process. Finally, osumilite also has broken down and formed orthopyroxene+cordierite+K-feldspar+quartz symplectite. Metamorphic evolution of the ultrahigh-temperature granulites from Bunt Island is summarized as follows: (1) near isothermal decompression from *c.* 1100 MPa to *c.* 900 MPa at *c.* 1050–1100°C in the sapphirine-quartz stability field, then (2) pressure and temperature decreasing (near isobaric cooling) in the garnet-cordierite stability field. Harley (1989) and many other authors suggested the isobaric cooling from peak *P-T* condition of the sapphirine+quartz stability field, while metamorphic evolution of two types of UHT-metamorphic rocks from Bunt Island indicates isothermal decompression from the peak UHT-condition as part of the clockwise *P-T* path.

Acknowledgments

We would like to sincerely thank all members of JARE-39 led by K. Shibuya and K. Moriwaki and to all crew members of the icebreaker *Shirase* for their help during the helicopter operation. We are also grateful to T. Tsujimori, Y. Yoshimura and T. Miyamoto for their collaboration in frequent discussions. Thanks are also due to E. S. Grew and K. K. Podolesskii for critical reading of the manuscript. T.H. and W.A.C. are also grateful to NIPR and UWA, respectively, for enabling them to carry out the field work. This work was partly supported by a Grant-in-Aid for Scientific Research from the Ministry of Education, Science, Sports and Culture, Japan (No. 09440176: Y. Osanai).

References

Aranovich, L.Ya and Berman, R.G. (1996): Optimized standard state and solution properties of minerals II. Comparisons, predictions, and applications. Contrib. Mineral. Petrol., **126**, 25–37.

Arima, M. and Barnett, R.L. (1984): Sapphirine bearing granulites from the Sipiwesk Lake area of the late Archean Pikwitonei granulite terrain, Manitoba, Canada. Contrib. Mineral. Petrol., **88**, 102–112.

Asami, M., Suzuki, K., Grew, E.S. and Adachi, M. (1998): CHIME ages for granulites from the Napier Complex, East Antarctica. Polar Geosci., **11**, 172–199.

Audibert, N., Bertrand, P., Hensen, B.J., Kienast, J.R. and Ouzegane, K. (1993): Cordierite-K-feldspar-quartz-orthopyroxene symplectite from southern Algeria: new evidence for osumilite in high-grade metamorphic rocks. Mineral. Mag., **57**, 354–357.

Carrington, D.P. and Harley, S.L. (1995): Partial melting and phase relations in high-grade metapelites: an experimental petrogenetic grid in the KFMASH system. Contrib. Mineral. Petrol., **120**, 270–291.

Clifford, T.N., Stumpfl, E.F., Burger, A.J., McCarthy, T.S. and Rex, D.C. (1981): Mineral-chemical and isotopic studies of Namaqualand granulites, South Africa: a Grenville analogue. Contrib. Mineral. Petrol., **77**, 225–250.

Dallwitz, W.B. (1968): Co-existing sapphirine and quartz in granulite from Enderby Land, Antarctica. Nature, **219**, 476–477.

Droop, G.T.R. and Bucher-Nurminen, K. (1984): Reaction textures and metamorphic evolution of sapphirine-bearing granulites from the Gruf Complex, Italian Central Alps. J. Petrol., **25**, 766–803.

Ellis, D.J. (1980): Osumilite-sapphirine-quartz granulites from Enderby Land, Antarctica: *P-T* conditions of metamorphism, implications for garnet-cordierite equilibria and the evolution of the deep crust. Contrib. Mineral. Petrol., **74**, 201–210.

Ellis, D.J., Sheraton, J.W., England, R.N. and Dallwitz, W.B. (1980): Osumilite-sapphirine-quartz granulites from Enderby Land, Antarctica: mineral assemblages and reactions. Contrib. Mineral. Petrol., **72**, 123–143.

Grew, E.S. (1980): Sapphirine+quartz association from Archaean rocks in Enderby Land, Antarctica. Am. Mineral., **65**, 821–836.

Grew, E.S. (1982): Osumilite in the sapphirine-quartz terrane of Enderby Land, Antarctica: implications for osumilite petrogenesis in the granulite facies. Am. Mineral., **67**, 762–787.

Harley, S.L. (1985): Garnet-orthopyroxene bearing granulites from Enderby Land, Antarctica: metamorphic pressure-temperature-time evolution of the Archaean Napier Complex. J. Petrol., **26**, 819–856.

Harley, S.L. (1987): A pyroxene-bearing meta-ironstone and other pyroxene-granulites from Tonagh Island, Enderby Land, Antarctica: further evidence for very high temperature (>980°C) Archaean regional metamorphism in the Napier Complex. J. Metamorph. Geol., **5**, 341–356.

Harley, S.L. (1989): The origin of granulites: a metamorphic perspective. Geol. Mag., **126**, 215–331.

Harley, S.L. (1998): On the occurrence and characterization of ultrahigh-temperature crustal metamorphism. What Drives Metamorphism and Metamorphic Reactions?, ed. by P.J. Treloar and P.J. O'Brien. London, Geological Soc., 81–107 (Geol. Soc. London Spec. Publ., 138).

Harley, S.L. and Hensen, B.J. (1990): Archaean and Proterozoic high-grade terranes of East Antarctica (40–80°E): A case study of diversity in granulite facies metamorphism. High-temperature Metamorphism and Crustal Anatexis, ed. by J.R. Ashworth and M. Brown. London, Unwin Hyman, 320–370 (Mineral. Soc. Ser., 2).

Harley, S.L. and Motoyoshi, Y. (2000): Al zoning in orthopyroxene in a sapphirine quartzite: evidence for >1120°C UHT metamorphism in the Napier Complex, Antarctica, and implications for the entropy of sapphirine. Contrib. Mineral. Petrol., **138**, 293–307.

Harley, S.L., Hensen, B.J. and Sheraton, J.W. (1990): Two-stage decompression in orthopyroxene-sillimanite granulites from Forefinger Point, Enderby Land, Antarctica: implications for the evolution of the Archaean Napier Complex. J. Metamorph. Geol., **8**, 591–613.

Hensen, B.J. and Harley, S.L. (1990): Graphycal analysis of *P-T-X* relations in granulite facies metapelites. High-temperature Metamorphism and Crustal Anatexis, ed. by J.R. Ashworth and M. Brown, London, Unwin-Hyman, 19–56 (Mineral. Soc. Ser., 2).

Hensen, B.J. and Motoyoshi, Y. (1992): Osumilite-producing reactions in high temperature granulites

from the Napier Complex, East Antarctica: Tectonic implications. Recent Progress in Antarctic Earth Science, ed. by Y. Yoshida *et al.* Tokyo, Terra Sci. Publ., 87–92.

Hokada, T., Osanai, Y., Toyoshima, T., Owada, M., Tsunogae, T. and Crowe, W.A. (1999): Petrology and metamorphism of sapphirine-bearing aluminous gneisses from Tonagh Island in the Napier Complex, East Antarctica. Polar Geosci., **12**, 49–70.

Holland, T.J.B. and Powell, R. (1998): An internally consistent thermodynamic data set for phases of petrological interest. J. Metamorph. Geol., **16**, 309–343.

Holland, T.J.B., Babu, E.V.S.S.K. and Waters, D.J. (1996): Phase relations of osumilite and dehydration melting in pelitic rocks: a simple thermodynamic model for the KFMASH system. Contrib. Mineral. Petrol., **124**, 383–394.

Horrocks, P.C. (1983): A corundum and sapphirine paragenesis from the Limpopo Mobile Belt, southern Africa. J. Metamorph. Geol., **1**, 13–23.

Ishizuka, H., Suzuki, S. and Kojima, H. (1995): Mineral paragenesis of the sapphirine-bearing rock from the Austkampane area of the Sør Rondane Mountains, East Antarctica. Proc. NIPR Symp. Antarct. Geosci., **8**, 65–74.

Ishizuka, H., Ishikawa, M., Hokada, T. and Suzuki, S. (1998): Geology of the Mt. Riiser-Larsen area of the Napier Complex, East Antarctica. Polar Geosci., **11**, 154–171.

Kamenev, E.N. (1975): The geology of Enderby Land. Acad. Sci. USSR Comm. Antarct. Res. Rep., 14.

Motoyoshi, Y. and Hensen, B.J. (1989): Sapphirine-quartz-orthopyroxene symplectites after cordierite in the Archaean Napier Complex, Antarctica: Evidence for a counterclockwise *P-T* path? Eur. J. Mineral., **1**, 467–471.

Motoyoshi, Y. and Matsueda, H. (1984): Archean granulites from Mt. Riiser-Larsen in Enderby Land, East Antarctica. Mem. Natl Inst. Polar Res., Spec. Issue, **33**, 103–125.

Motoyoshi, Y., Hensen, B.J. and Matsueda, H. (1990): Metastable growth of corundum adjacent to quartz in a spinel-bearing quartzite from the Archaean Napier Complex, Antarctica. J. Metamorph. Geol., **8**, 125–130.

Motoyoshi, Y., Hensen, B.J. and Arima, M. (1993): Experimental study of the high-pressure stability limit of osumilite in the system K_2O-MgO-Al_2O_3-SiO_2: implications for high-temperature granulites. Eur. J. Minaral., **5**, 439–445.

Motoyoshi, Y., Ishikawa, M. and Fraser, G.L. (1994): Reaction textures in granulites from Forefinger Point, Enderby Land, Antarctica: an alternative interpretation on the metamorphic evolution of the Rayner Complex. Proc. NIPR Symp. Antarct. Geosci., **7**, 101–114.

Motoyoshi, Y., Ishikawa, M. and Fraser, G.L. (1995): Sapphirine-bearing silica-undersaturated granulites from Forefinger Point, Enderby Land, Antarctica: evidence for a clockwise *P-T* path? Proc. NIPR Symp. Antarct. Geosci., **8**, 121–129.

Osanai, Y., Owada, M., Kagami, H., Hamamoto, T. and Hensen, B.J. (1996): Sapphirine granulite and related high *P-T* metamorphic rocks from Highland Complex, Sri Lanka. Gondwana Res. Group Misc. Publ., **4**, 107–108.

Osanai, Y., Hamamoto, T., Maishima, O. and Kagami, H. (1998): Sapphirine-bearing granulites and related high-temperature metamorphic rocks from the Higo metamorphic terrane, west-central Kyushu, Japan. J. Metamorph. Geol., **16**, 53–66.

Osanai, Y., Toyoshima, T., Owada, M., Tsunogae, T., Hokada, T. and Crowe, W.A., (1999): Geology of ultrahigh-temperature metamorphic rocks from Tonagh Island in the Napier Complex, East Antarctica. Polar Geosci., **12**, 1–28.

Osanai, Y., Toyoshima, T., Owada, M., Tsunogae, T., Hokada, T., Yoshimura, Y., Miyamoto, T., Motoyoshi, Y., Crowe, W. A., Harley, S.L., Kanao, M. and Iwata, M. (2001): Geological map of Tonagh Island, Antarctica. Antarctic Geological Map Series, Sheet 38 (with explanatory text 34p.). Tokyo, National Institute of Polar Research.

Owada, M., Osanai, Y. and Kagami, H. (1994): Isotopic equilibration age of Sm-Nd whole-rock system in the Napier Complex (Tonagh Island), East Antarctica. Proc. NIPR Symp. Antarct. Geosci., **7**, 122–132.

Owada, M., Osanai, Y., Toyoshima, T., Tsunogae, T., Hokada, T. and Crowe, W.A. (1999): Petrography and geochemistry of mafic and ultramafic rocks from Tonagh Island in the Napier Complex, East

Antarctica: a preliminary report. Polar Geosci., **12**, 87–100.

Owada, M., Osanai, Y., Tsunogae, T., Hamamoto, T., Kagami, H., Toyoshima, T. and Hokada, T. (2001): Sm-Nd garnet ages of retrograde garnet bearing granulites from Tonagh Island in the Napier Complex, East Antarctica: A preliminary report. Polar Geosci., **14**, 75–87.

Pattison, D.R.M. and Tracy, R.J. (1991): Phase equilibria and thermobarometry of metapelites. Rev. Mineral., **26**, 105–206.

Sandiford, M.A. (1985): The metamorphic evolution of granulites at Fyfe Hills: implications for Archaean crustal thickness in Enderby Land, Antarctica. J. Metamorph. Geol., **3**, 155–178.

Sengupta, P., Karmakar, S., Dasgupta, S. and Fukuoka, M. (1991): Petrology of spinel granulites from Araku, Eastern Ghats, India, and a petrogenetic grid for sapphirine-free rocks in the system FMAS. J. Metamorph. Geol., **9**, 451–459.

Sheraton, J.W. (1980): Geochemistry of Precambrian metapelites from East Antarctica: secular and metamorphic variation. BMR J. Aust. Geol. Geophys., **5**, 279–288.

Sheraton, J.W., Offe, L.A., Tingey, R.J. and Ellis, D.J. (1980): Enderby Land, Antarctica- an unusual Precambrian high-grade metamorphic terrain. J. Geol. Soc. Aust., **27**, 1–18.

Sheraton, J.W., Tingey, R.J., Black, L.P., Offe, L.A. and Ellis, D.J. (1987): Geology of Enderby Land and Western Kemp Land, Antarctica. BMR Bull., **223**, 51 p.

Shiraishi, K., Ellis, D.J., Fanning, C.M., Hiroi, Y., Kagami, H. and Motoyoshi, Y. (1997): Re-examination of the metamorphic and protolith ages of the Rayner Complex, Antarctica: evidence for the Cambrian (Pan-African) regional metamorphic event. The Antarctic Region: Geological Evolution and Processes, ed. by C.A. Ricci. Siena, Terra Antarct. Publ., 79–88.

Suzuki, S., Hokada, T., Ishikawa, M. and Ishizuka, H. (1999): Geochemical study of granulites from Mount Riiser-Larsen, Enderby Land, East Antarctica: Implication for protoliths of the Archaean Napier Complex. Polar Geosci., **12**, 101–125.

Yoshimura, Y., Motoyoshi, Y., Grew, E.S., Miyamoto, T., Carson, C.J. and Dunkley, D.J. (2000): Ultrahigh-temperature metamorphic rocks from Howard Hills in the Napier Complex, East Antarctica. Polar Geosci., **13**, 60–85.

(Received March 12, 2001; Revised manuscript accepted June 1, 2001)